AD-A050 919 SRI INTERNATIONAL MENLO PARK CA F/G 9/5
RANDOM GAIN AND PHASE ERROR EFFECTS IN OPTIMAL ARRAY STRUCTURES--ETC(U)
SEP 77 C W JIM, L J GRIFFITHS N00014-75-C-0930
UNCLASSIFIED NL

| OF |
AD
A050919

END
DATE
FILMED
4-78
DDC

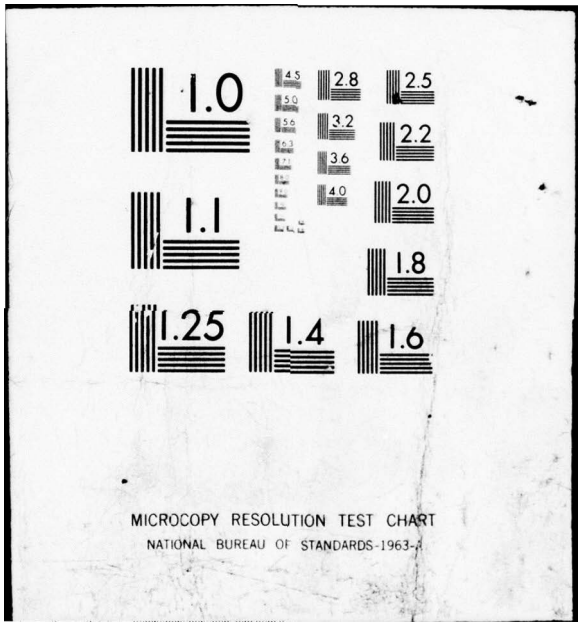
1.0
1.1
1.25
1.4
1.6
1.8
2.0
2.2
2.5
2.8
3.2
3.6
4.0
4.5
5.0
5.6
6.3
7.1
8.0
MICROCOPY RESOLUTION TEST CHART
NATIONAL BUREAU OF STANDARDS-1963-A

The views and conclusions contained in this document are those of the authors and should not be interpreted as necessarily representing the official policies, either expressed or implied, of the U.S. Air Force or the U.S. Government.

Technical Report EE 77-2 *September 1977*

RANDOM GAIN AND PHASE ERROR EFFECTS IN OPTIMAL ARRAY STRUCTURES

By: C. W. JIM L. J. GRIFFITHS
Department of Electrical Engineering
University of Colorado

Prepared for:

ELECTRONIC SYSTEMS DIVISION (AFSC)
USAF 414L SYSTEM PROGRAM OFFICE
HANSCOM AFB, MASSACHUSETTS 01731

through

SRI International
333 Ravenswood Avenue
Menlo Park, California 94025

SRI International Subcontract 14107
under
CONTRACT N00014-75-C-0930
(NR 088-076)

This research was sponsored by the Electronic Systems Division, Air Force Systems Command, through an SRI International subcontract, and was monitored by the Office of Naval Research under Contract No. N00014-75-C-0930 (NR 088-076).

Approved by:

L. J. GRIFFITHS, *Project Director*
University of Colorado

SECURITY CLASSIFICATION OF THIS PAGE (When Data Entered)

REPORT DOCUMENTATION PAGE

READ INSTRUCTIONS BEFORE COMPLETING FORM

1. REPORT NUMBER

2. GOVT ACCESSION NO.

3. RECIPIENT'S CATALOG NUMBER

4. TITLE (and Subtitle)

RANDOM GAIN AND PHASE ERROR EFFECTS IN OPTIMAL ARRAY STRUCTURES.

5. TYPE OF REPORT & PERIOD COVERED

Technical Report, EE 77-2 Covering the Period 1 October 76 to 31 May 77

6. PERFORMING ORG. REPORT NUMBER

EE 77-2

7. AUTHOR(s)

Charles W. Jim Lloyd J. Griffiths

8. CONTRACT OR GRANT NUMBER(s)

SRI International Subcontract 14107 under prime N00014-75-C-0930 new

9. PERFORMING ORGANIZATION NAME AND ADDRESS

University of Colorado
Department of Electrical Engineering
Boulder, Colorado 80302

10. PROGRAM ELEMENT, PROJECT, TASK AREA & WORK UNIT NUMBERS

ONR NR 088-076

11. CONTROLLING OFFICE NAME AND ADDRESS

Electronic Systems Division (AFSC)
USAF 414L System Program Office
Hanscom AFB, Massachusetts 01731

12. REPORT DATE

Sep 1977

13. NO. OF PAGES

45 p.

14. MONITORING AGENCY NAME & ADDRESS (if diff. from Controlling Office)

Office of Naval Research (Code 461(FP))
800 North Quincy Street
Arlington, Virginia 22217

15. SECURITY CLASS. (of this report)

UNCLASSIFIED

15a. DECLASSIFICATION/DOWNGRADING SCHEDULE

N/A

16. DISTRIBUTION STATEMENT (of this report)

Approved for public release; distribution unlimited.

17. DISTRIBUTION STATEMENT (of the abstract entered in Block 20, if different from report)

18. SUPPLEMENTARY NOTES

This research was sponsored by the Electronic Systems Division, Air Force Systems Command, through an SRI Subcontract, and was monitored by the Office of Naval Research under Contract N00014-75-C-0930 (NR 088-076).

19. KEY WORDS (Continue on reverse side if necessary and identify by block number)

Optimal array processor
Least-mean-square procedures
Sidelobe cancellation
Antenna beamforming
Optimal beamforming
Random errors in beamformers

20. ABSTRACT (Continue on reverse side if necessary and identify by block number)

This report summarizes a quantitative analysis of the effects of random gain and phase errors and angular variations on the performance of a class of Least-Mean-Square (LMS) optimal array processors. Two different structures for the LMS optimal array processor were studied. Both belong to a general class of side-lobe cancelling arrays and both structures employed a conventional beamformer as an integral part of the structure. The first implemented a linear constraint using software and the second employed a simple spatial hardware preprocessor to

(continued)

DD FORM 1 JAN 73 1473

EDITION OF 1 NOV 65 IS OBSOLETE

SECURITY CLASSIFICATION OF THIS PAGE (When Data Entered)

410 281

19. KEY WORDS (Continued)

20 ABSTRACT (Continued)

implement the same constraint. An analysis of the sensitivity of both LMS optimal array processors as well as a conventional beamformer to random gain and phase errors was performed. It was found that the two optimal processors had identical error sensitivity, provided that certain conditions on the spatial hardware preprocessor were met. Findings also indicated that the optimal array processors were more sensitive to input errors than the conventional processor but nevertheless offered significant interference rejection improvements over conventional beamforming methods in the presence of these errors. It was shown that degradations due to random gain and phase errors could be restored to some extent by increasing the number of temporal/spatial degrees-of-freedom (DOF) in the optimal beamformers.

CONTENTS

TABLES

ILLUSTRATIONS

I INTRODUCTION

Recent results have demonstrated that the use of receive-array beamforming systems which are designed to be "optimal" in the sense of rejecting noise and interference offer superior performance over conventional beamforming methods in HF applications. The purpose of this report is to offer a quantitative analysis of the effects of random fluctuations in the received waveforms on the overall performance of optimal beamformers. These fluctuations are the result of signal distortion imposed by ionospheric reflection as well as the presence of system noise in the receive-array electronics. In this report, we assume that signal distortion affects both gain and phase of each spatially-propagated waveform received by the elements. Thus, the effects of gain and phase errors on both the desired or target signal as well as directional interferers are considered. In the case of phase errors on the desired signal, we consider two separate cases: 1) the zero-mean case in which the average direction of arrival of the target signal coincides with the pointing direction of the array and 2) non-zero mean cases in which the mean arrival direction is other than expected. In the latter case, the desired signal is treated as an interfering signal by the processor and may suffer some amplitude degradation at the beamformed output. Quantitative predictions of this effect as a function of the offset angle are presented in section IV of this report. Comparisons with conventionally-weighted beamforming systems are also presented for all cases studied.

Previous studies relating to the effects of random gain and phase errors have largely been restricted to the case of conventional beamforming systems. (See Ruze [1], Rondinelli [2], and Green, et. al. [3])

Carver, et.al., [4] have studied the effects of beam-pointing errors in planar phased arrays and recent work by McDonough [5] has shown the effects of random input errors on the directivity of both conventional and linearly-constrained optimal beamformers. The work presented in this report augments that of McDonough in that two different optimal structures are analyzed herein and specific calculations of noise rejection and beam patterns are presented.

In section II, we describe the conventional and optimal beamforming structures of interest in this work. The latter are termed noise-cancelling beamformers and utilize auxiliary beamforming subsystems designed to cancel undesired interference which is present in the conventional array output. The specific model used to compute the effects of random errors is described in detail in Section III. Briefly, we model each spatially propagated signal incident on the array as having been transmitted to the array by a random channel. The characteristics of this channel then determine the nature of the phase and gain errors observed at the element outputs. Simulation results based on this model are presented in Section IV and Section V contains summary and conclusions drawn from the study.

II BEAMFORMING STRUCTURES

The general form of the receiving array stem of interest in this work is shown in Fig. 1. Each array element contains a separate receiver which converts the HF element signals to baseband. In practice, subarrays may serve as elements for each individual receiver [6,7] and the individual receivers are gain and phase matched across the bandwidth of the transmitted signal. The baseband outputs are then simultaneously sampled and digitized prior to beamforming. A sampling rate greater than twice the receiver bandwidth is used to prevent aliasing and all beamforming is carried out using a real-time digital processor. We assume that the receivers shown in Fig. 1 contain steering delays which pre-point the array system to the assumed direction of the desired signal. Thus, in an ideal system, if $x_i(k)$ is used to represent the k-th sample from the i-th receiver output,

$$x_i(k) = s(k) + n_i(k) \tag{1}$$

where $s(k)$ is the desired signal and $n_i(k)$ is the total of all noise and interference observed at the i^{th} element. Of course, in practical systems, the presence of system and propagation errors will cause the $s(k)$ term in Eq. (1) to be a function of element number i.

Conventional beamforming consists of gain weighting the receiver samples $x_i(k)$ to produce a beamformed output $y_c(k)$ given by

$$y_c(k) = \sum_{i=1}^{K} W_{ci} X_i(k) \tag{2}$$

where W_{ci} is the i-th conventional weight.

Optimal beamforming structures employ a beamformer which utilizes delayed samples from each receiver. These processors have been proposed

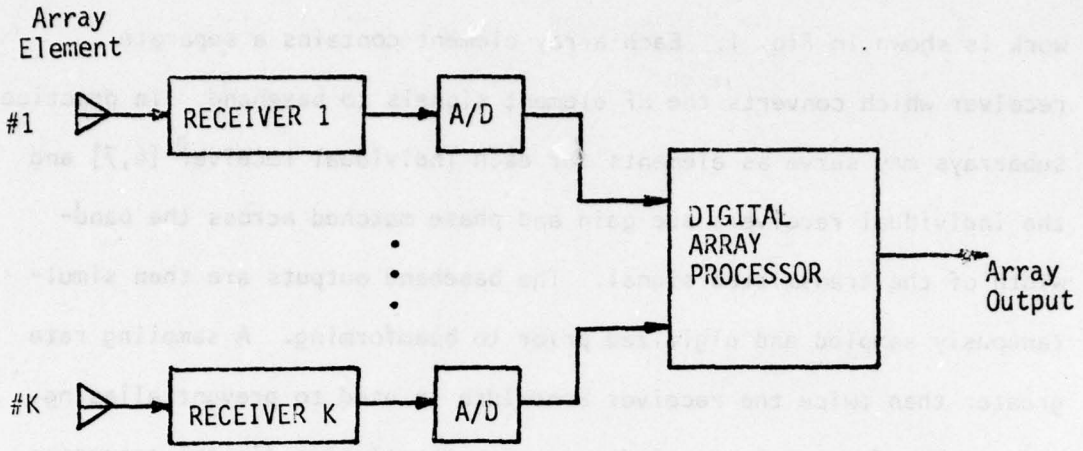

Figure 1. Digital Antenna Array System Model

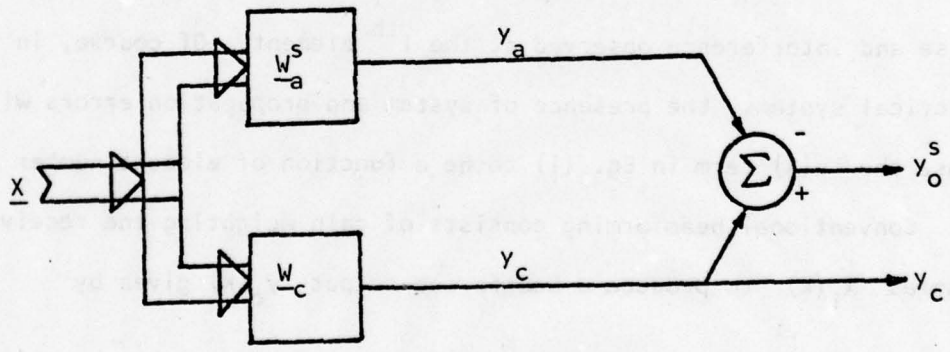

Figure 2. Software-constrained noise-cancelling optimal array structure.

in a variety of forms and have been widely discussed in the literature [6-11]. The specific structures of interest in this work have been termed noise-cancelling or side-lobe-cancelling array structures [12,13]. Within this class we consider two distinct implementations termed software-constrained (Fig. 2) and hardware-constrained (Fig. 3).

Software-Constrained Optimal Beamformer

In the software-constrained system, a conventional beam output $y_c(k)$ is formed in a manner identical to that shown in Eq. (3) except for the presence of a bulk time-delay of 1/2 samples. Thus,

$$y_c(k) = \sum_{i=1}^{K} w_{ci} x_i(k-L/2) \tag{3}$$

The reason for the delay will be explained shortly. A noise-cancelling auxiliary beam $y_a^S(k)$ is formed from a weighted sum of delayed signals from each of the receivers. A total of L samples from each element are combined using the multichannel digital filter shown in Fig. 4.

In matrix notation, we denote the vector of KL auxiliary weights $\underline{W}_a^S$ as

$$\underline{W}_a^S = \begin{bmatrix} \underline{w}_{1,1}^S \\ \vdots \\ \underline{w}_{1,L}^S \\ \vdots \\ \underline{w}_{k,1}^S \\ \vdots \\ \underline{w}_{k,L}^S \end{bmatrix} \tag{4}$$

These weights multiply a vector of delayed receiver signals $\underline{X}(k)$ defined by

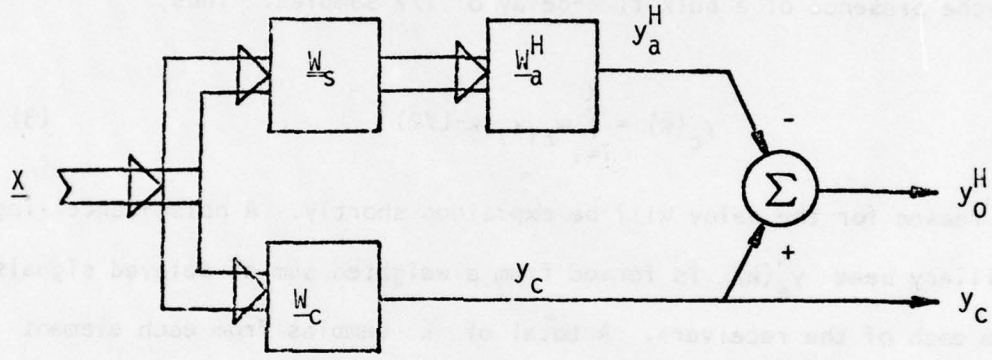

Figure 3. Hardware constrained noise-cancelling optimal array structure

$$\underline{X}(k) = \begin{bmatrix} x_1(k) \\ \vdots \\ x_1(k-L+1) \\ \vdots \\ x_K(k) \\ \vdots \\ x_K(k-L+1) \end{bmatrix} \tag{5}$$

The auxiliary beam output $y_a(k)$ is then

$$y_a(k) = \underline{X}^T(k)\underline{W}_a^S \tag{6}$$

In noise-cancelling array structures, an optimal weight set $\underline{W}_a^S$ is found such that the output noise and interference power is minimized subject to the constraint that the desired signal passes undistorted through the processor. Since the desired signal is presumed to be in-phase at each receiver output--Eq.(1)--this can be accomplished by constraining each column of weights in the processor shown in Fig. 4 to sum to zero. Thus we require

$$\sum_{i=1}^{K} w_{i,j}^S = 0 \quad , \quad j = 1,2,\ldots L \tag{7}$$

or, in matrix notation using T to denote transpose,

$$\underline{\underline{C}}^T\underline{W}_a^S = 0 \tag{8}$$

where $\underline{\underline{C}}$ is a KL by K symmetric matrix of ones and zeros defined by

$$\underline{\underline{C}} = \begin{bmatrix} \underline{1} & \underline{0} & \underline{0} & . & . \\ \underline{0} & \underline{1} & \underline{0} & & \\ . & & . & & \\ . & & & . & \\ & & & & \underline{1} \end{bmatrix} \tag{9}$$

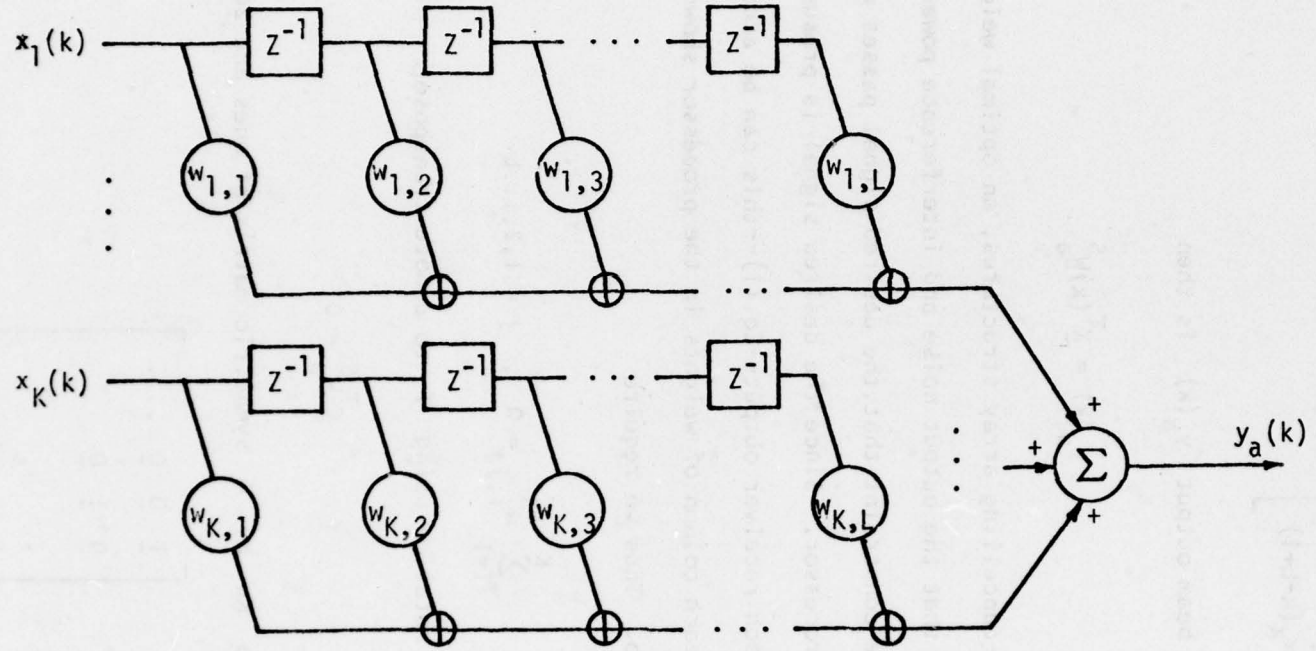

Figure 4. Multichannel Digital Filter

In this expression, $\underline{1}$ and $\underline{0}$ have been used to denote column vectors of ones and zeros, respectively.

Once the weighting coefficients have been constrained by Eq. (8)--termed here the software constraint--the ideal signal cannot appear in the auxiliary beamformed output. Minimum output noise and interference is then achieved by finding $\underline{W}_a^S$ such that the difference beam $y_o^s(k)$ in Fig. 2 has minimum power subject to the constraint in Eq. (8). Frost [14] has given an excellent discussion of this problem and the resulting solution. As discussed in [6,7], inserting a delay of L/2 in the conventional beam places the phase reference of the conventional beamformed signal in the center of the auxiliary processor. (Note that if L is odd, L/2 is replaced by (L-1)/2). This phase shift has been shown experimentally to offer the best overall performance in practical implementations of noise-cancelling arrays.

In order to obtain a convenient expression for the form of the optimal weights $\underline{W}_a^S$, we defined a KL-dimensional conventional beamforming vector $\underline{W}_c$ as

$$\underline{W}_c = \begin{bmatrix} \underline{0} \\ \underline{0} \\ \vdots \\ w_{c1} \\ \vdots \\ w_{ck} \\ \underline{0} \\ \vdots \\ \underline{0} \end{bmatrix} \tag{10}$$

The optimal weights are then given by [11, 14]

$$\underline{W}_a^S = \underline{W}_c - \underline{\underline{R}}_x^{-1}\underline{\underline{C}}(\underline{\underline{C}}^T\underline{\underline{R}}_x^{-1}\underline{\underline{C}}_x)^{-1}\underline{\underline{C}}^T\underline{W}_c \tag{11}$$

where $\underline{\underline{R}}_x$ is the KL x KL matrix of space/time correlations observed at the receiver outputs. Specifically,

$$\underline{\underline{R}}_x \triangleq E\,[\underline{X}(k)\underline{X}^T(k)] \tag{12}$$

where $E[\cdot]$ denotes expectation.

In practical applications of this beamformer such as those discussed by Kelly, et.al. [11], the correlation matrix is computed using time averages of observed receiver output. For example, the correlation between the signal from element i delayed by ℓ units and that from element j delayed by m units is approximated by

$$r_{i,j}(\ell,m) = \frac{1}{T_o} \sum_{k=1}^{T_o} x_i(k-\ell)x_j(k-m) \tag{13}$$

where T_o is the observation interval. For the purposes of the present study, we assume that averages of this or an equivalent type have been carried out with sufficient data to accurately estimate the elements of $\underline{\underline{R}}_x$. This matrix is in turn used to compute $\underline{W}_a^S$ using Eq. (11)

Hardware-Constrained Optimal Beamformer

Figure 3 shows an alternate implementation of the sidelobe-cancelling optimal array structure. The only difference between this and the software-constrained beamformer in Fig. 2 is the use of a spatial preprocessing matrix $\underline{\underline{W}}_s$ which converts the vector of received signals $\underline{X}(k)$ into a modified vector $\underline{X}'(k)$. The auxiliary beam $y_a^H(k)$ is formed as a weighted sum of the elements of $\underline{X}'(k)$ using a multichannel filter similar to that shown in Fig. 4. The purpose $\underline{\underline{W}}_s$ is to block the desired signal $s(k)$ from $\underline{X}'(k)$ where

$$\underline{X}'(k) = \underline{\underline{W}}_S \underline{X}(k) \tag{14}$$

is a $K'L$ dimensional vector of modified receiver signals $(K' < K)$.

Inspection of Eq's (1), (5), and (14) shows that $s(k)$ will be successfully blocked if $\underline{\underline{W}}_S$ is constructed as a diagonal matrix of identical $K' \times K$-dimensional submatrices $\underline{\underline{w}}_S$,

$$\underline{\underline{W}}_S = \begin{bmatrix} \underline{\underline{w}}_S & \underline{\underline{0}} & \underline{\underline{0}} & \cdots & \underline{\underline{0}} \\ \underline{\underline{0}} & \underline{\underline{w}}_S & \underline{\underline{0}} & & \\ & \ddots & & & \\ & & \ddots & & \\ & & & & \underline{\underline{w}}_S \end{bmatrix} \tag{15}$$

where $\underline{\underline{0}}$ is used to represent a $K \times K$ matrix of zeros. In effect, implementing the preprocessor in the form shown in Eq. (15) is equivalent to applying a spatial prefilter $\underline{\underline{w}}_S$ to the set of K received array signals $\{x_i(k)\}$, and $s(k)$ is blocked provided that the rows of $\underline{\underline{w}}_S$ sum to zero.

Two examples of spatial preprocessors for the case where $K = 8$ are shown in Fig. 5. In Fig. 5a, $K' = 4$ and $\underline{\underline{w}}_S$ is given by

$$\underline{\underline{w}}_S = \begin{bmatrix} 1 & -1 & 0 & . & . & . & . & 0 \\ 0 & 0 & 1 & -1 & 0 & . & . & . \\ . & . & . & 0 & 1 & -1 & 0 & 0 \\ 0 & . & . & . & . & 0 & 1 & -1 \end{bmatrix}. \tag{16}$$

Alternately, in Fig. 5b, $K' = 7$ and

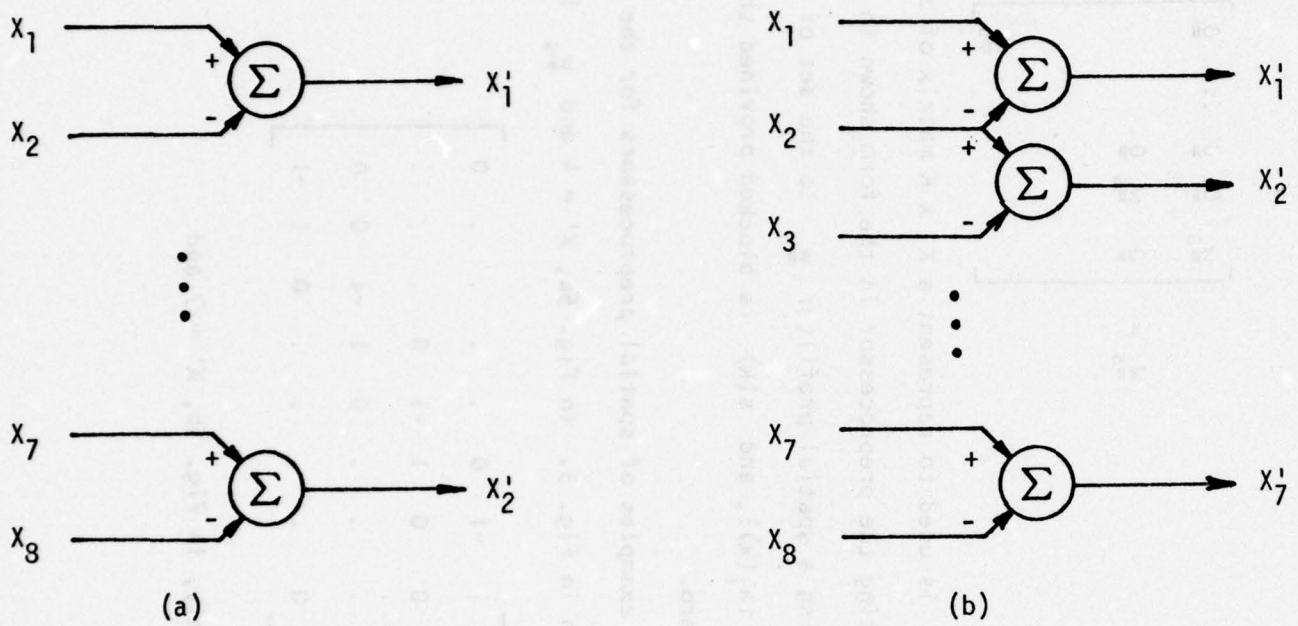

Figure 5. Two Simple Spatial Filter Structures, (a) 4-Element and (b) 7-Element

$$\underline{\underline{W}}_s = \begin{bmatrix} 1 & -1 & 0 & 0 & 0 & 0 & 0 & 0 \\ 0 & 1 & -1 & 0 & 0 & 0 & 0 & 0 \\ 0 & 0 & 1 & -1 & 0 & 0 & 0 & 0 \\ 0 & 0 & 0 & 1 & -1 & 0 & 0 & 0 \\ 0 & 0 & 0 & 0 & 1 & -1 & 0 & 0 \\ 0 & 0 & 0 & 0 & 0 & 1 & -1 & 0 \\ 0 & 0 & 0 & 0 & 0 & 0 & 1 & -1 \end{bmatrix} \tag{17}$$

Other forms of spatial preprocessors which successfully block the desired signal are possible and discussed further in the sections following.

Given that $\underline{X}'(k)$ does not contain $s(k)$--i.e. the desired signal has been blocked by the hardware preprocessor--minimum output noise and interference is achieved by finding $\underline{W}_a^H$ such that the difference beam $y_0^H(k)$ in Fig. 3 has minimum power. The equation for the auxiliary beam $y_a^H(k)$ in matrix notation is

$$y_a^H(k) = \underline{X}^T(k)\underline{\underline{W}}_s^T\underline{W}_a^H \tag{18}$$

and the resulting optimal weights $\underline{W}_a^H$ are given by

$$\underline{W}_a^H = (\underline{\underline{W}}_s^T\underline{\underline{R}}_x\underline{\underline{W}}_s)^{-1}\ \underline{\underline{W}}_s^T\underline{\underline{R}}_x\underline{W}_c \tag{19}$$

A complete derivation of this result is presented in Appendix A. It should be noted that the correlation matrix $\underline{\underline{R}}_x$ which appears in (19) is identical to that defined by Eq's (12) and (13) for the software-constrained beamformer.

Discussion

It has been demonstrated [11, 15] that the optimal software and hardware auxiliary beamformers shown in Figs. 2 and 3 and defined by

Eq's (11) and (19), respectively, are identical provided that the spatial matrix $\underline{\underline{W}}_S$ is of rank K-1. Equivalently, $K' = K-1$ and the rows of $\underline{\underline{W}}_S$ must be linearly independent. One may interpret this hardware constraint preprocessor as a set of K' beamformers, each having a null in the direction of the desired signals. Methods for encoding additional constraints into the preprocessor are discussed in Reference [12] and [13].

III MODEL USED FOR GAIN AND PHASE PERTURBATIONS

The formulation presented in the previous section for optimal array structures assumes that the desired signal is a plane wave incident on the receive array from a known direction. Under these conditions, optimal array processing can be shown to provide significant improvement in the rejection of undesired directional interference when the interference consists of plane waves propagating uniformly across the array. However, when the target signal comes from other than steered direction, the optimal processor may regard the signal as interference and present some degree of rejection of the desired signal. In addition, some degradation of performance may result due to amplitude and phase fluctuations of all spatially propagated signals. The purpose of this section is to present a model which can be used to quantitatively determine the effects of these errors on the overall performance of both forms of the optimal processor.

In the following, we will assume a stationary environment and model the amplitude and phase variations as zero-mean random processes. The effect of an error in the assumed direction of arrival of the desired signal is included by assuming a non-zero mean for the phase errors. For simplicity, this mean corresponds to plane-wave propagation from other than the desired direction and performance degradation is measured as a function of angular offset, or tilt, of the desired signal. In addition, it is further assumed that the antenna array consists of K elements distributed in a line at equispaced intervals. The direction of arrival of the desired signal is perpendicular to the array and is termed the boresight direction.

Model and Assumptions

To simplify the following presentation, the case of a single spatially-propagating desired signal and a single directional interference is first considered. The model formulation is then extended to the case of multiple signals and interferences.

Figure 6 shows the signal, noise and interference model for the simple case. Two spatially coherent signals are present: a desired target signal, $s(t)$, and a directional interference, $n(t)$. They are modeled as zero-mean, random and uncorrelated processes, and are assumed to be sinusoidal with random phases. Two independent, identically distributed channels denoted by g_0 and g_1 in Figure 6 are used to model the effects of random amplitude and phase fluctuations. Thus, the output signals $\tilde{s}(t)$, $\tilde{n}(t)$ contain random errors and propagate toward the receiving array in the form of distorted plane waves. To illustrate the channel model consider the target signal shown in Figure 6. For a complex signal representation, we have

$$s(t) = \sigma_s e^{j(\omega_o t+\phi_s)} \tag{20}$$

where σ_s and ω_o are the amplitude and demodulated frequency, respectively, of the desired signal. The phase term ϕ_s is modelled as a uniform random variable over a 2π interval. The power content of this signal is given by

$$E[|s(t)|^2] = \sigma_s^2 \tag{21}$$

The random channel adds both gain and phase modulation to this signal and produces an output $\tilde{s}(t)$ given by

$$\tilde{s}(t) = c_s[1+a(t)]\sigma_s e^{j[\omega_0 t+\phi_s-\theta(t)]} \tag{22}$$

Both amplitude and phase variation terms $a(t)$ and $\theta(t)$ are modelled as independent, zero-mean, gaussian processes with variances σ_a^2 and σ_θ^2 respectively. The scalar term c_s is included to preserve invariance of the input-out power of the channel and is given by

$$c_s = \frac{1}{\sqrt{1+\sigma_a^2}} \tag{23}$$

The time behavior of $a(t)$ is modelled as white--i.e. wide band--and $\theta(t)$ is assumed to be constant over the time interval during which correlations are measured. Each array element is presumed to receive an $\tilde{s}(t)$ which results from a separate channel which is independent of the other array elements. In effect, this model assumes that amplitude variation are uncorrelated spatially and rapidly time varying but that the phase variations are spatially decorrelated and nearly constant in time at each element. Assumptions identical to these have been used by Lee and Waterman [16] to accurately model millimeter wave propagation through the atmosphere.

Thus, after propagation through the i-th channel, the sampled signal $\tilde{s}_i(k)$ observed at the output of the i-th receiver is given by

$$\tilde{s}_i(k) = c_s[1+a_i(k)]\ \sigma_s e^{j[\omega_0 k+\phi_s-\theta_i(k)]} \tag{24}$$

The generalized spatial/tempral correlation element defined by Eq. (13) is then modelled for the signal only and (assuming $i \neq j$) as

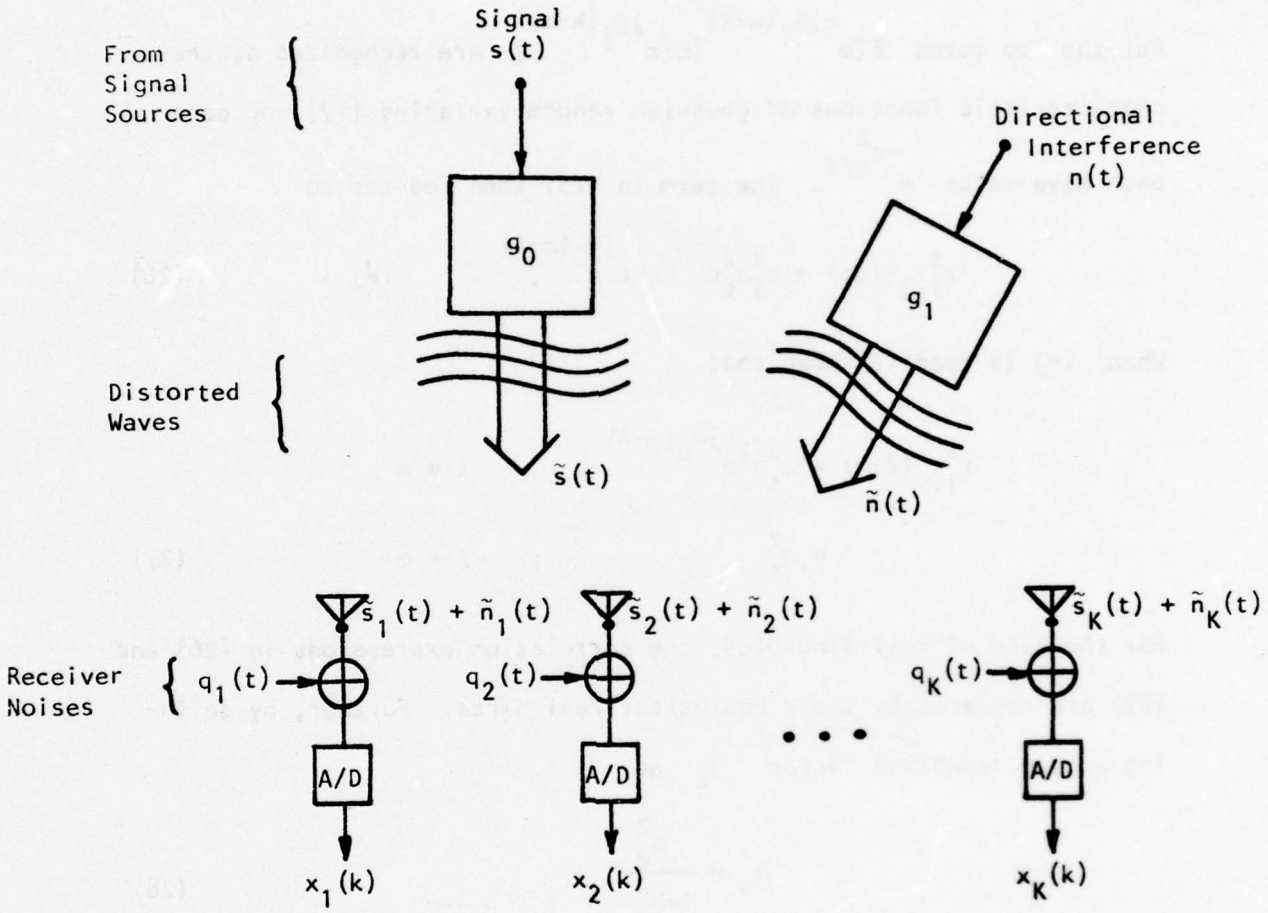

Figure 6. The signal, noise and interference model

$$r^s_{i,j}(\ell,m) = E[\tilde{s}_i(k-\ell)\tilde{s}^*_j(k-m)] = E[\tilde{s}_i(k-\ell)]E[\tilde{s}^*_j(k-m)]$$

$$= c_s\sigma_s e^{j(\omega_0 k-\omega_0\ell+\phi_s)} E[e^{-j\theta_i(k-\ell)}]$$

$$\cdot\, c_s\sigma_s e^{-j(\omega_0 k-\omega_0 m+\phi_s)} E[e^{j\theta_j(k-m)}] \qquad (25)$$

But the two terms $E[e^{-j\theta_i(k-\ell)}]E[e^{j\theta_j(k-m)}]$ are recognized as the characteristic functions of gaussian random variables [17] and each each have value $e^{-\sigma^2_\theta/2}$. The term in (25) then reduces to

$$r^s_{i,j}(\ell,m) = c_s^2\sigma_s^2 e^{-\sigma^2_\theta} e^{j\omega_0(m-\ell)}, \qquad i\neq j \qquad (26)$$

When i=j is readily shown that

$$r^s_{i,i}(\ell,m) = c_s^2\sigma_s^2 e^{j\omega_0(m-\ell)}, \quad \ell \neq m$$

$$= \sigma_s^2, \quad \ell = m \qquad (27)$$

For the case of real sinusoids, the correlation expressions in (26) and (27) are replaced by their equivalent real parts. Further, by defining a gain reduction factor α_a as

$$\alpha_s = \frac{\sigma_a^2}{1+\sigma_a^2} \qquad (28)$$

and using (23), the resulting spatial/temporal correlation functions for a real signal may be expressed as

$$r^s_{i,j}(\ell,m) = \sigma_s^2(1-\alpha_a)e^{-\sigma^2_\theta}\cos[\omega_0(m-\ell)], \quad i \neq j \qquad (29)$$

$$r^s_{i,i}(\ell,m) = \sigma_s^2(1-\alpha_a)\cos[\omega_0(m-\ell)], \quad \ell \neq m$$

$$=\sigma_s^2, \quad \ell = m \qquad (30)$$

Discussion

The development presented above in Eq's (24)-(30) has shown how correlation values for the desired signal may be computed from the random channel model shown in Fig. 6 and described by Eq's (22) and (23). For a directional interference, analagous calculations are carried out. The only difference in this case is that the random phase term $\theta_i(k)$ in (24) is modeled as having a non-zero mean $\bar{\theta}_i$ corresponding to the average direction of arrival of the interfering wavefront. The term $E[e^{-j\theta_i(k-\ell)}]$ in (25) then becomes [17] $e^{j\bar{\theta}_i} e^{-\sigma_\theta^2/2}$, and $\bar{\theta}_i$ represents the average phase delay to the i-th array element. Spatial/temporal correlation values for a directional interferer similar to those in Eq's (29) and (30) are then given by

$$r^n_{i,j}(\ell,m) = \sigma_n^2(1-\alpha_a)e^{-\alpha_\theta^2}\cos[w_0(m-\ell)+\bar{\theta}_j-\bar{\theta}_i] \quad , \quad i \neq j \qquad (31)$$

$$r^n_{i,i}(\ell,m) = \sigma_n^2(1-\alpha_a)\cos[\omega_0(m-\ell)] \quad , \quad \ell \neq m$$

$$= \sigma_n^2 \quad , \quad \ell = m. \qquad (32)$$

The random channel model is readily extended to the case of multiple directional interferers and/or multiple target signals by modeling these sources as statistically independent. In this case, the net correlation function is the sum of appropriate signal and noise terms similar to those given above.

Inspection of the correlation terms in Eq's (25) and (31) shows that the effect of the gaussian amplitude and phase noise in the system is to reduce the amount of inter element correlation. For the amplitude model, this reduction term is $(1-\alpha_a)$ and for phase noise it becomes $e^{-\sigma_\theta^2}$. The latter is a direct consequence of the

gaussian assumption and changes as other statistical models are used. For example, if a uniform probability density on phase is used with zero mean and variance σ^2, the term is given by a sine function $\sin(\sqrt{3}\sigma_\theta)/\sqrt{3}\sigma_\theta$.

Because the model reduces the measured spatial correlation values, one would expect a reduction in the amount of improvement offered by optimal arrays to be more comparable with that provided by conventional beamformers. In the limit of complete spatial decorrelation it is readily shown that optimal and conventional processors have identical performance. Examples presented in the section following illustrate this degradation for the case of a simple line array of eight equally-spaced elements.

IV SIMULATION RESULTS

In this section, we present some simulation which illustrate the sensitivity of a line array to random gain and phase errors. The simulations were carried out using the CDC 6400 facility at the University of Colorado Boulder campus. A receiving array of eight elements was chosen and a raised-cosine window was selected for the conventional beamformer. The optimal beamformers are characterized in terms of number of spatial and temporal degrees of freedom (DOF) in the auxiliary beamforming path. Thus, a four element auxiliary channel with four taps per delay line is indicated by 4 x 4 DOF.

Input Signal and Noise Fields

Two cases were considered. Case (i) consisted of a single target signal and one directional interference, and case (ii) consisted of multiple target signals and interferences. In both cases, uncorrelated receiver noises were added to the inputs and the total power input normalized to unity at each element. The angle of arrival for all directional sources was measured in terms of a normalized spatial angle θ chosen in the range of $-\pi$ to π. An angular increment of 2π radians corresponds to the spatial fold-over angle of the linear array. This angle is generally referred to as the gratinglobe separation and the actual angle in a practical array depends on the element separation and HF carrier frequency [6]. The received frequency f used for the simulations is presented on a normalized scale of 0 to 0.5 with 0.5 representing one-half of the sampling frequency.

Table I summarizes the details of the input waveforms. The signal-to-interference ratio (SIR) and the signal-to-total-noise ratio (STR) observed at each element were defined as follows:

TABLE I

SUMMARY OF INPUT WAVEFORM CHARACTERISTICS

(a) Single Target Signal Example

Target Signal			Interference			Receiver Noise
Power	f	θ	Power	f	θ	Power
0.02	.25	0	.88	.20	0.4	0.1

$(SIR)_{in} = -16.43dB$

(b) Multiple Target Signal Example

Target Signal			Interference			Receiver Noise
Power	f	θ	Power	f	θ	Power
0.01	0.225	0	0.3	0.2	0.4	0.1
0.01	0.25	0	0.3	0.3	-0.4	
0.01	0.275	0	0.3	0.4	0.6	

$(SIR)_{in} = -14.77$ dB

$$(SIR)_{in} = \frac{\text{total input power of all target signals}}{\text{total input power of all directional interference}}$$

$$(STR)_{in} = \frac{\text{total input power of all target signals}}{\text{total input power of directional interference and receiver noise}}$$

An evaluation of the performance observed with these examples was performed and is summarized below. As discussed in Section II above, the software and hardware constrained beamformers are identical when the spatial preprocessing matrix $\underline{\underline{W}}_S$ (see Fig. 3) produces K-1 independent outputs. In the comparisons which follow, then, any optimal beamforming structure which is characterized as having 7 x L DOF applies in both optimal structures. If, on the other hand, K' x L DOF are used and K' < 7 then the results apply only to the hardware constrained case. To quantitatively measure the performance of the array structures of interest in the presence of random gain and phase errors, four criteria were selected. These were:

A. Main-Lobe Gain Reduction: The gain reduction in the main lobe direction was computed as the ratio of output target signal power under random perturbations to that under no perturbation. Figure 7 illustrates this parameter as a function of both the amplitude noise variance reduction factor α, Eq. (28), and the standard deviation of the phase noise σ_θ for the case (i) model. Both signal and directional noise were assumed to have the same degree of random gain and phase perturbation. The 7 x 4 DOF case applies to both hardware and software constrained optimal beamformers while the 4 x 4 DOF examples refers only to the hardware constrained structure.

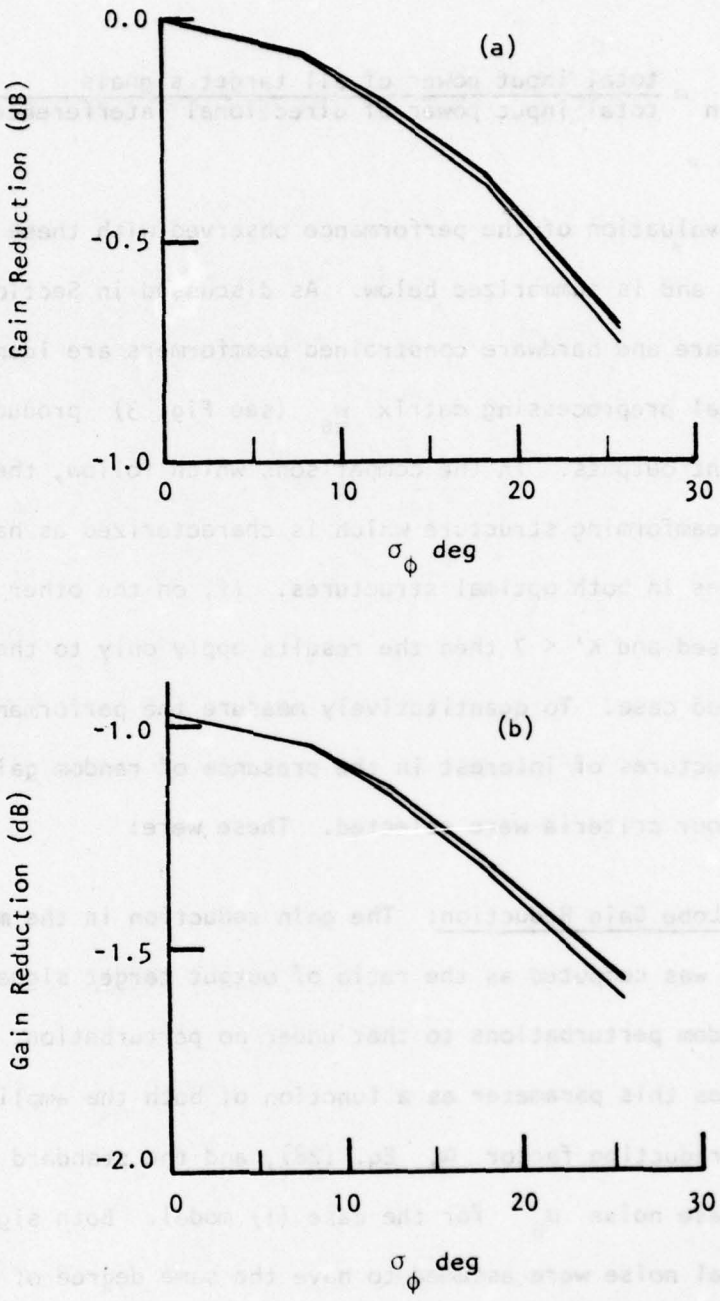

Figure 7. Main-lobe gain reduction for case (i).

(a) $\alpha = 0.0$ and (b) $\alpha = 0.2$

B. Interference and Noise Rejection: The degree to which noise and interference are rejected was measured by computing the signal-to-interference ratio SIR and signal-to-total-noise ratio STR observed at the beamformed output of a particular structure. These quantities were defined as follows:

$$\text{SIR} \triangleq \frac{\text{total target signal output power}}{\text{total directional interference output power}}$$

$$\text{STR} \triangleq \frac{\text{total target signal output power}}{\text{total interference and noise output power}}$$

Results obtained for the cases studied are summarized in Fig. 8 through 11.

C. Rejection of Target Signal: Figure 12 shows the effect observed in SIR and STR when the mean angle of arrival of the target signal was other than boresight. These curves measure the penalty incurred when the array is miss-pointed. Angular tilts of 0 to $0.3\,\pi$ radians were investigated. In the three-component example --i.e. case (ii)-- all three target signals were assumed to have the same offset angle. It should be noted that the shape of the conventional beamformer response in these curves is identical with the beam pattern of the conventionally-weighted array.

Additional responses of this type are presented in Fig. 13 for case (ii) as a function of the amount of gain noise. In these plots the STR values have been normalized to their boresight values to better illustrate the degree of rejection achieved. Similar behavior was observed for the case (i) example.

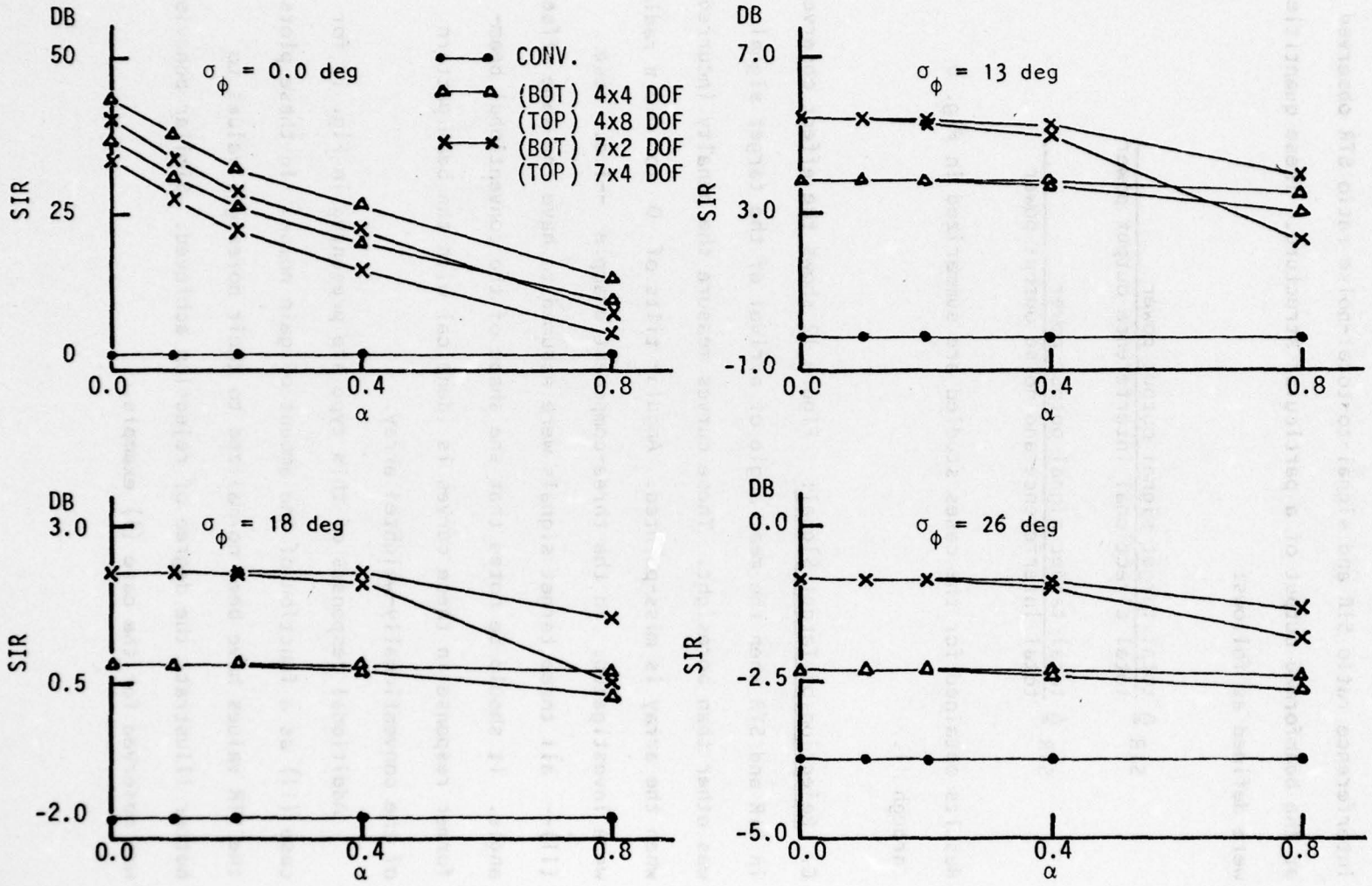

Figure 8. SIR vs. gain reduction (α) and phase noise variance for case (i).

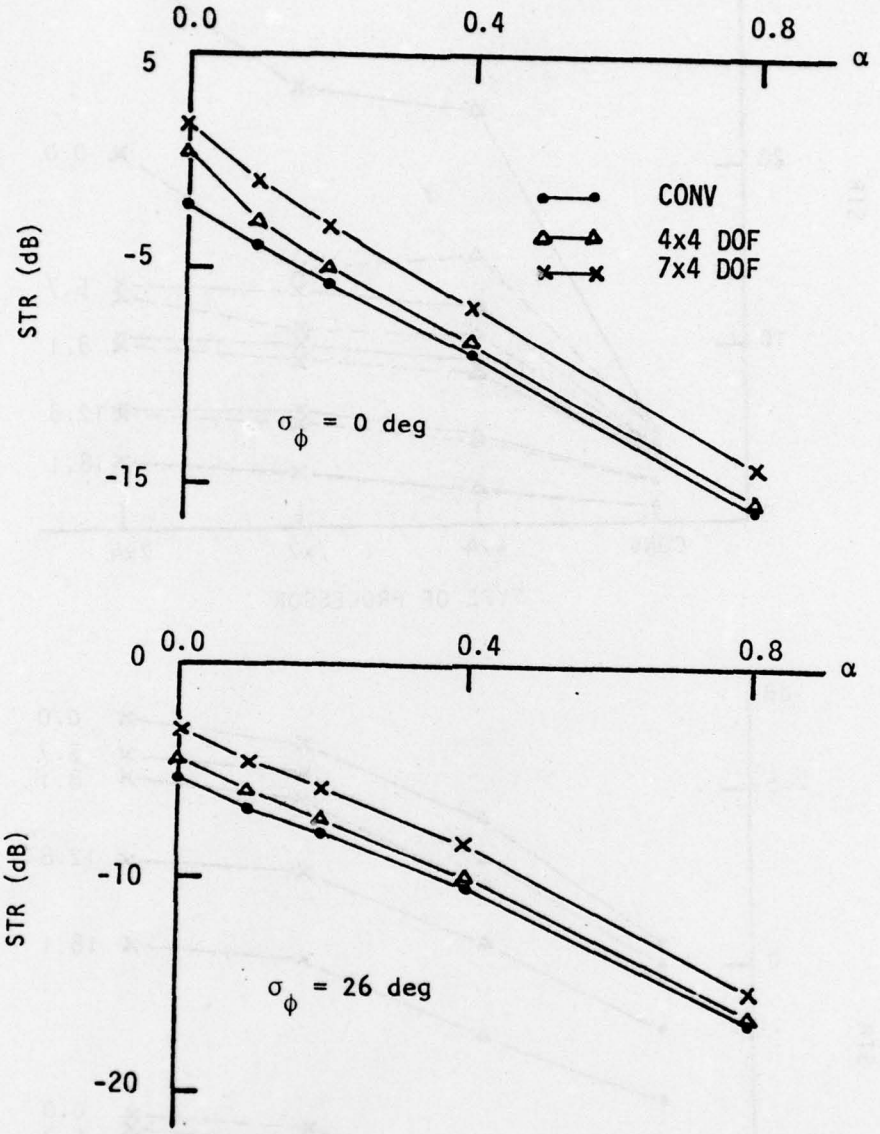

Figure 9. STR vs. gain reduction (α) and phase noise variance for case (i).

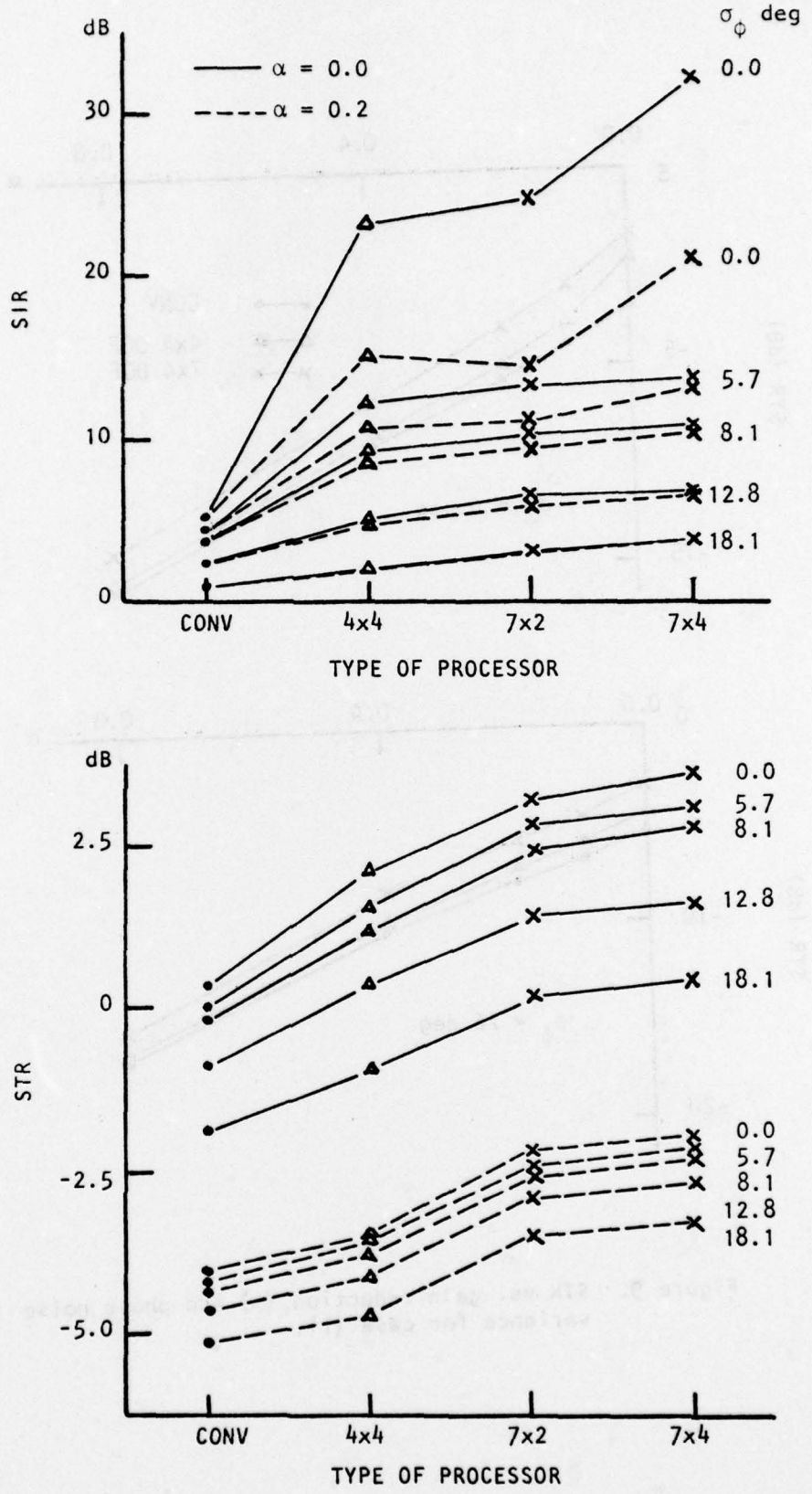

Figure 10. Interference and noise rejection behavior under gain and phase variation for case (ii).

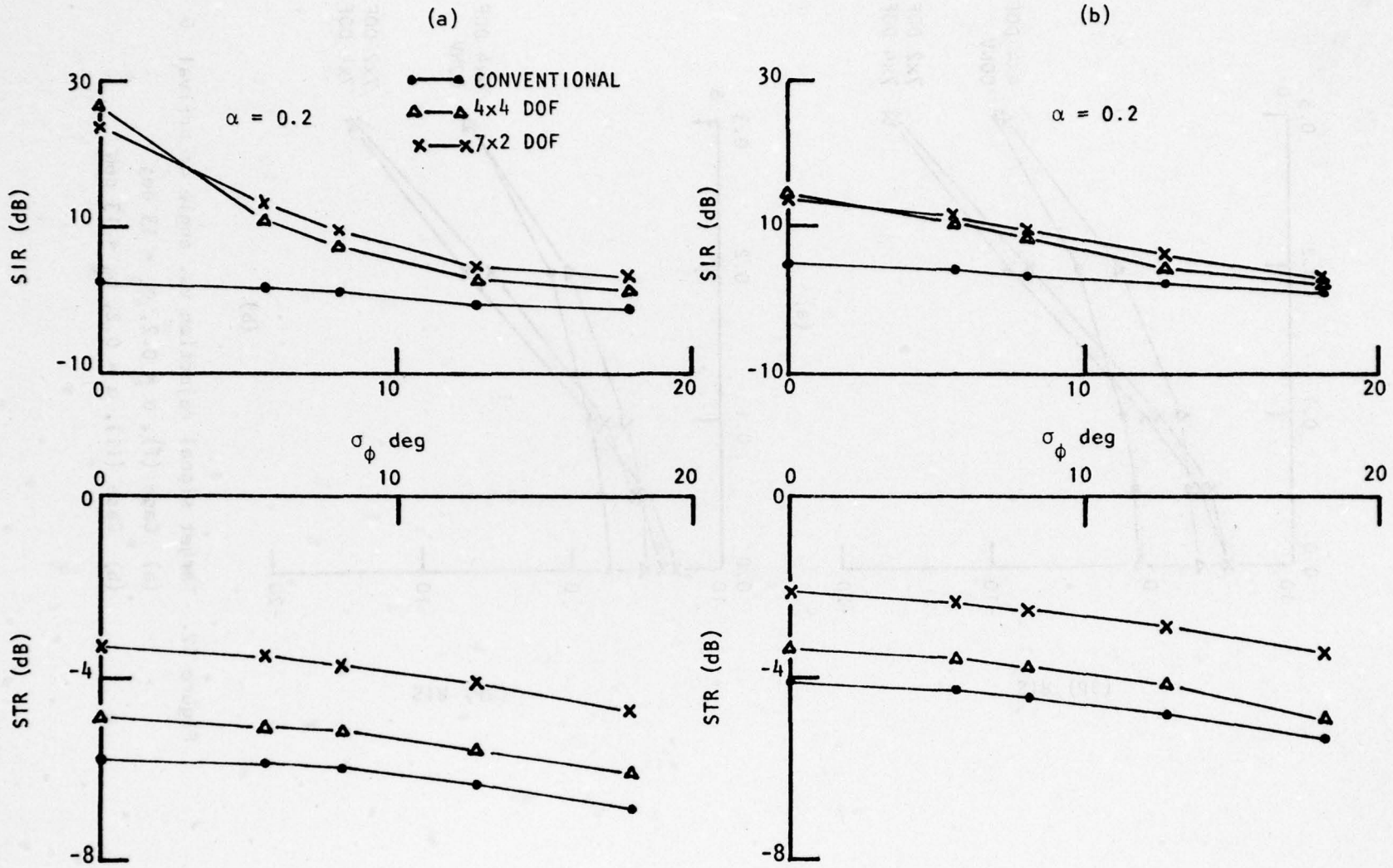

Figure 11. Comparison of interference and noise rejection behavior, (a) case (i) and (b) case (ii).

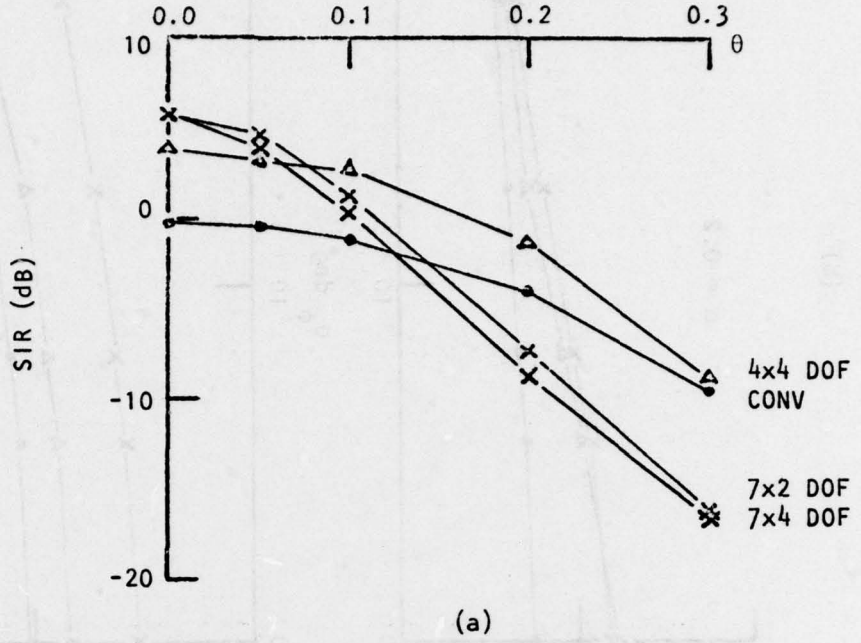

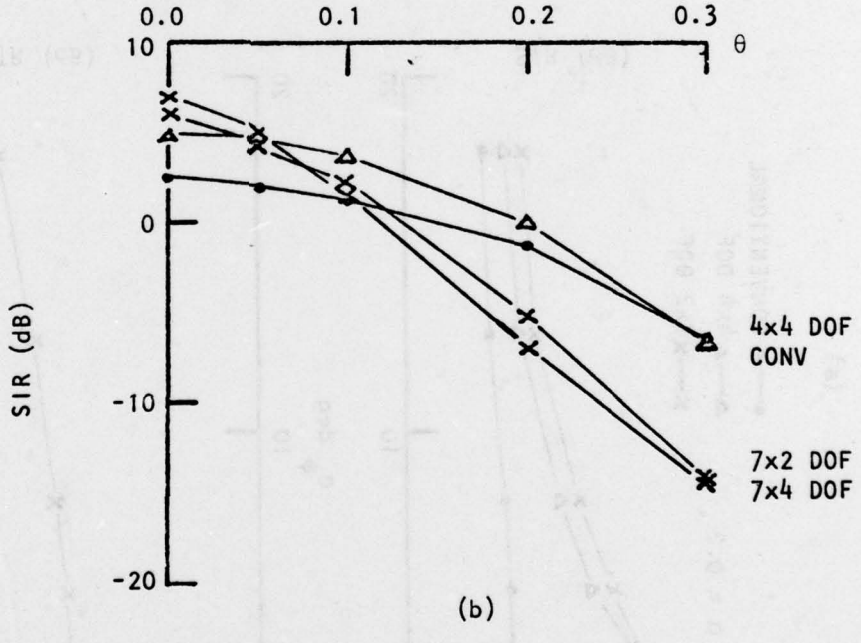

Figure 12. Target signal rejection vs. angle of arrival θ

(a) Case (i), $\alpha = 0.2$, $\sigma_\phi = 13$ deg

(b) Case (ii), $\alpha = 0.2$, $\sigma_\phi = 13$ deg

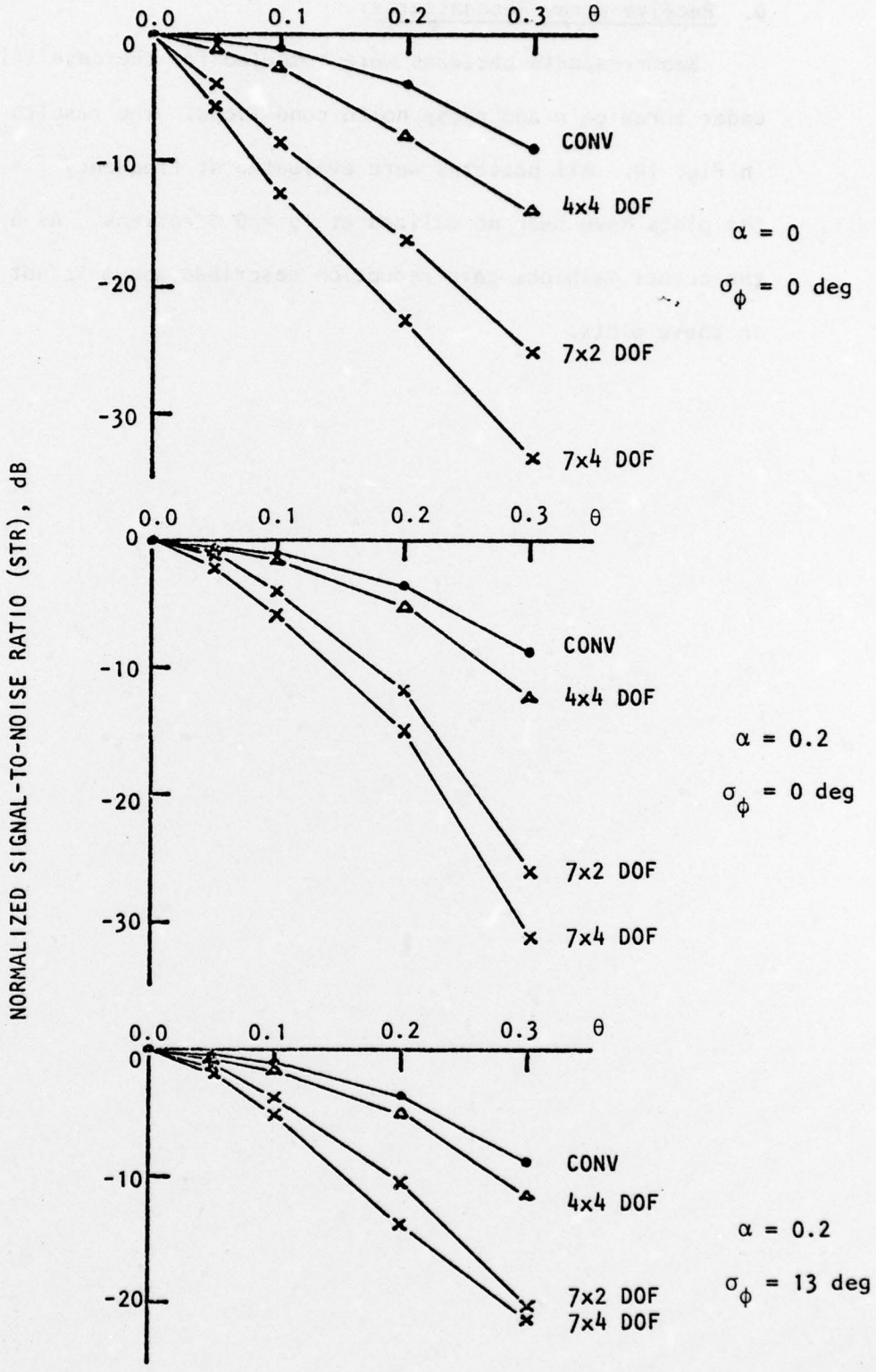

Figure 13. Target signal rejection vs. angle of arrival for case (ii) normalized to the boresight response.

D. Receive-array Beampatterns:

Beam-response patterns were computed for the case (ii) example under three gain and phase noise conditions. The results are shown in Fig. 14. All patterns were evaluated at frequency f = 0.25 and the plots have been normalized at $\theta = 0\ \pi$ radians. As a result, the actual mainlobe gain reduction described above is not evident in these plots.

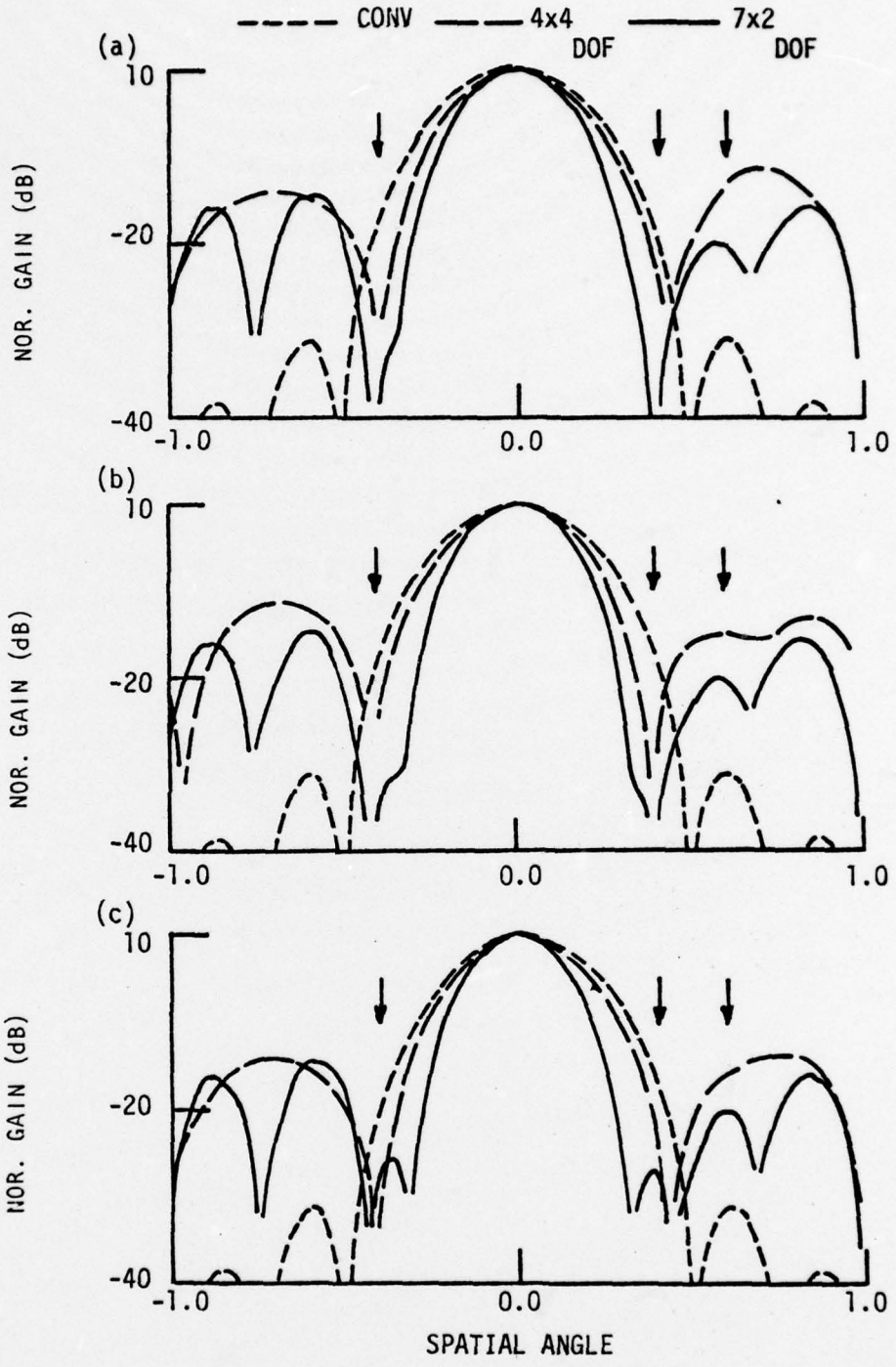

Figure 14. Comparison of receiving array beam-pattern for case (ii).

(a) $\alpha = 0.0$, $\sigma_\phi = 0.0$ deg

(b) $\alpha = 0.0$, $\sigma_\phi = 13$ deg

(c) $\alpha = 0.2$, $\sigma_\phi = 13$ deg

(interference noises indicated by down-pointed arrows)

V DISCUSSION AND CONCLUSIONS

A random channel model has been formulated and presented which allows investigation of the sensitivity of beamforming structures to random gain and phase perturbations in the input waveforms. Procedure for computing the appropriate space/time correlation values of the received signals have been given. These allow direct computation of the sensitivity of any least-mean-square criterion optimal beamformer. Two specific optimal structures were studied, each belonging to the sidelobe cancelling array class. The conclusions drawn from this study are as follows:

1. Optimal array processing offers significant interference rejection improvement over conventional beamforming even at large gain and phase error levels.
2. Performance degradation of optimal processors is largely dominated by random phase errors.
3. The performance of the hardware constrained optimal beamformer in the presence of random fluctuations is identical to that of the software constrained structure provided that the maximum possible spatial degrees of freedom are employed. All attempts to reduce the number of spatial degrees of freedom below this level in the hardware constrained processor led to poorer performance.
4. Increasing the temporal degrees of freedom in the optimal processor (i.e., the number of taps on each delay line) had no obvious effect on the performance of the processor in the presence of random fluctuation.
5. Beam patterns computed for optimal beamformers show narrower

widths of the mainlobe when greater numbers of spatial degrees of freedom are used in the auxiliary channel. In addition, these patterns exhibit wider null depths in the presence of phase noise.

APPENDIX A

To derive Equation (19), a cost function is defined as follows:

$$H(\underline{W}_a) = \frac{1}{2} E[y_o^2]$$

$$= \frac{1}{2} (\underline{W}_c - \underline{\underline{W}}_s^T \underline{W}_a)^T \underline{\underline{R}}_x \underline{\underline{W}}_c - \underline{\underline{W}}_s^T \underline{W}_e) \quad , \tag{A.1}$$

a factor of 1/2 is included to simplify later arithmetic.

Taking the gradient of (A.1),

$$\nabla H(\underline{W}_a) = -\underline{\underline{W}}_s^T \underline{\underline{R}}_x (W_c - \underline{\underline{W}}_s^T \underline{W}_a) \tag{A.2}$$

Letting

$$\nabla H(\underline{W}_a) = 0$$

then

$$\underline{\underline{W}}_s \underline{\underline{R}}_x \underline{\underline{W}}_s^T \underline{W}_a = \underline{\underline{W}}_s^T \underline{\underline{R}}_x \underline{\underline{W}}_c \tag{A.3}$$

Assuming $\underline{\underline{R}}_x$ is positive definite, it can be shown that the inverse of the transformed matrix $(\underline{\underline{W}}_s \underline{\underline{R}}_x \underline{\underline{W}}_s^T)$ exists. Then the optimal solution of $\underline{W}_a$ is,

$$\underline{W}_a \text{ opt} = (\underline{\underline{W}}_s \underline{\underline{R}}_x \underline{\underline{W}}_s^T)^{-1} \underline{\underline{W}}_s^T \underline{\underline{R}}_x \underline{\underline{W}}_c \tag{A.4}$$

which is the resulting optimal formula (19).

REFERENCES

(1) J.R. Ruze, "Physical Limitations on Antennas," Technical Report #248 Research Laboratory of Electronics, Massachusetts Institute of Technology, 1952.

(2) L.A. Rondinelli, "Effects of Random Errors on the Performance of Antenna Arrays of Many Elements," I.R.E. National Conference Record, Part I, pp. 175-189, 1959.

(3) C.A. Greene and R.T. Moller, "The effect of normally distributed random phase errors on synthetic array gain patterns," IEEE Trans. Military Electronics, pp. 130-139, April 1962.

(4) K.R. Carver, W.E. Cooper, and W.L. Stutzman, "Mean pointing errors of planar-phased arrays," IEEE Trans. Antennas and Propagation, vol. AP-21, pp. 199-202, March 1973.

(5) R.N. McDonough, "Degraded performance of nonlinear array processors in the presence of data modeling errors," J. Acoust. Soc. Amer., vol. 51, pp. 1186-1193, April 1972.

(6) T.W. Washburn and L.E. Sweeney, Jr., "An on-line adaptive beamforming capability for HF backscatter radar," IEEE Trans. Antennas and Propagation, vol. AP-24, September 1976.

(7) L.J. Griffiths, "Time-domain adaptive beamforming of HF backscatter radar signals," IEEE Trans. Antennas and Propagation, vol. AP-24, Sept. 1976.

(8) M. Backus, J. Burg, D. Baldwin, and E. Bryan, "Wideband extraction of mantel P waves from ambient noise," Geophysics, vol. 29, pp. 672-692, October 1964.

(9) J.P. Burg, "Three dimensional filtering with an array of seismometers," Geophysics, vol. 29, pp. 693-713, October 1964.

(10) Claerbout, "Detection of P waves from vector sources at great distances," Geophysics, vol. 29, pp. 197-211, April 1964.

(11) J. Kelly, Jr. and M.J. Levin, "Signal parameter estimator for seismometer arrays," Mass. Inst. Technol. Lincoln Lab. Tech. Rept. 339, January 1964.

(12) N.W. Owsley, "A recent trend in adaptive spatial processing for sensor arrays: Constrained adaptation;: Signal Processing, Proc. NATO ASI, J.W.R. Griffiths, P.L. Stocklin, and C. Van Schoonveld, (Eds.), Academic Press, 1973.

(13) L.J. Griffiths, "An adaptive noise-cancelling procedure for multidimensional systems," Proc. Asilomar Circuits and System Conference, Asilomar, Calif., Nov. 1976.

(14) O.L. Frost, III, "An algorithm for linearly constrained adaptive array processing," Proc. IEEE, vol. 60, pp. 926-935, August 1972.

(15) C.W. Jim, "Sensitivity comparisons for two classes of optimal array processors," Masters Thesis, Dept. of Elec. Eng., Univ. of Colo., Boulder, Colo., Aug. 1976.

(16) R.W. Lee and A.T. Waterman, Jr., "A large array for millimeter wave propagation studies," Proc. IEEE, vol. 54, no. 4, pp. 454-458, April 1966.

(17) A. Papoulis, Probability, Random Variables and Stochastic Processes, McGraw-Hill, Inc., New York, 1965.